

Phase boundary of a cubic superconducting circuit in a magnetic field of arbitrary magnitude and direction

Chia-Ren Hu and Chen-Hong Huang

Center for Theoretical Physics, Department of Physics, Texas A&M University, College Station, Texas 77843-4242

(Received 4 October 1990)

An exact analytic expression for the mean-field phase boundary $T_c(\mathbf{H})$ of a cubic superconducting circuit in an arbitrary external-magnetic-field vector \mathbf{H} is derived. The phase boundary of this circuit is shown to depend in a complex and sensitive way on both the magnitude and the direction of the magnetic field. Some practical applications of these properties are also suggested.

A large number of experimental¹ and theoretical² papers have now been published on the phase boundaries of superconducting networks of various geometries in an external magnetic field. Almost all of these papers considered *two-dimensional* networks in a perpendicular magnetic field, perhaps because so far only two-dimensional networks of various geometries have been conveniently fabricated in the laboratories using lithography techniques. A few of the above-cited theoretical papers³ have touched upon some properties of three-dimensional regular (i.e., latticelike) networks, but the main purposes of those papers were not to systematically study the phase boundary of three-dimensional networks in an arbitrary magnetic field vector. Thus in those discussions the applied magnetic field was restricted to a single principal direction of the network. Recently, Jeffery *et al.*⁴ pointed out that random *three-dimensional* networks may be used to model the reproducible oscillatory behavior in the microwave-absorption spectrum of high- T_c ceramic superconductors and other granular superconductors. To illustrate their idea they have studied several physical properties, viz., magnetoconductance, magnetization, and susceptibility, of one regular finite cubic network and one random finite network in certain directions of the applied magnetic field. But their approach is cruder than the Ginzburg-Landau theory (in the sense that they did not allow the magnitude of the superconducting order parameter to vary in the networks) and they did not study the phase boundaries of those networks. Three-dimensional superconducting networks *with prescribed geometric and physical characteristics* may be more difficult to fabricate in the laboratory than two-dimensional networks of similar characteristics, but once made they will have the additional interesting property that their phase boundaries will not only depend nontrivially on the magnitude of the applied magnetic field, but also on its direction, which we believe will have some applicational value. (See some suggestions near the end of this paper.) Thus in this paper we present a systematic study of the phase boundary of one of the simplest and most fundamental three-dimensional finite superconducting network, viz., a cubic superconducting circuit made of 12 superconducting straight line segments of identical length and cross-sectional area, in an applied magnetic

field of *arbitrary magnitude and direction*. [As in most previous studies of superconducting networks^{2,4} we assume that the lateral dimensions of the links are small in comparison with their superconducting coherence length $\xi(T)$.] This particular finite network we have chosen to study here is sufficiently simple to allow us to obtain exact analytic solution, so we can present a more thorough and accurate study of the dependence of the phase boundary on the magnitude and direction of the applied magnetic field.

In the mean-field (i.e., Ginzburg-Landau-de Gennes) approach to the normal-superconducting phase boundaries of thin superconducting-wire networks, each strand is assumed to obey a linearized one-dimensional Ginzburg-Landau equation, which may be solved in closed form. After enforcing a certain set of boundary conditions first derived by de Gennes,² at the nodes of the network, one then obtains a set of equations governing the values of the order parameter at the nodes, and having the structure of a generalized eigenvalue problem.² In the case when all of the strands have the same cross-sectional area and physical characteristics, the equation corresponding to the node i reads

$$\Delta_i \sum_j \cot[L_{ij}/\xi(T)] = \sum_j \Delta_j e^{i\gamma_{ij}} / \sin[L_{ij}/\xi(T)],$$

where Δ_i is the value of the (complex) superconducting order parameter at the i th node (or vertex) of the network, L_{ij} is the length of the strand (or link) connecting the node i with the node j , $\xi(T) = \xi(0)(1 - T/T_{c0})^{-1/2}$ is the temperature-dependent Ginzburg-Landau coherence length of the superconducting material that the strands are made of, with T_{c0} being the zero-field transition temperature of the superconducting material used, and also the transition temperature of the network at no applied field. $\gamma_{ij} \equiv (2\pi/\Phi_0) \int_i^j \mathbf{A} \cdot d\mathbf{l}$, with \mathbf{A} the vector potential, and $\Phi_0 (\equiv hc/2e)$ the flux quantum; the integral being along the strand connecting the nodes i and j , in the direction from i to j . The summation " \sum_j " is over all nodes j which are linked to the node i . Clearly we have as many equations as the number of nodes in the network which must be solved as coupled equations. The temperature T may be considered as the generalized eigenvalue

of this set of equations, and the transition temperature $T_c(\mathbf{H})$ should be identified as the largest among all such generalized eigenvalues. For the case when all links of the network are of equal length (i.e., all $L_{ij}=L$) and every node is connected to the same number Z of "nearest-neighbor" nodes, the above generalized eigenvalue problem further reduces to an ordinary eigenvalue problem, with $Z \cos[L/\xi(T)]$ being the eigenvalue (after multiplying both sides of the resultant equations by the

same constant factor $\sin[L/\xi(T)]$). Note that the highest T_c also corresponds to the largest $Z \cos[L/\xi(T)]$, so it is the largest eigenvalue we want in this case.

In the present problem of a cubic superconducting circuit of length a on each side, $Z=3$, and there are eight equations corresponding to the eight nodes which may be combined into a single matrix equation:

$$\begin{pmatrix} -\lambda & 1 & 1 & 0 & 1 & 0 & 0 & 0 \\ 1 & -\lambda & 0 & e^{-i\gamma n_x} & 0 & e^{i\gamma n_y} & 0 & 0 \\ 1 & 0 & -\lambda & 1 & 0 & 0 & 1 & 0 \\ 0 & e^{i\gamma n_x} & 1 & -\lambda & 0 & 0 & 0 & e^{i\gamma n_y} \\ 1 & 0 & 0 & 0 & -\lambda & 1 & e^{i\gamma n_z} & 0 \\ 0 & e^{-i\gamma n_y} & 0 & 0 & 1 & -\lambda & 0 & e^{i\gamma(n_z-n_x)} \\ 0 & 0 & 1 & 0 & e^{-i\gamma n_z} & 0 & -\lambda & 1 \\ 0 & 0 & 0 & e^{-i\gamma n_y} & 0 & e^{-i\gamma(n_z-n_x)} & 1 & -\lambda \end{pmatrix} \begin{pmatrix} \Delta_1 \\ \Delta_2 \\ \Delta_3 \\ \Delta_4 \\ \Delta_5 \\ \Delta_6 \\ \Delta_7 \\ \Delta_8 \end{pmatrix} = 0, \quad (1)$$

where $\lambda \equiv 3 \cos[a/\xi(T)]$ is the eigenvalue; $n_x \equiv \sin\alpha \cos\beta$, $n_y \equiv \sin\alpha \sin\beta$, and $n_z \equiv \cos\alpha$ are the directional cosines describing the direction of the applied magnetic field \mathbf{H} relative to the axes of the cube, with α and β the polar angles of \mathbf{H} , so that $\mathbf{H} = H(n_x \hat{e}_x + n_y \hat{e}_y + n_z \hat{e}_z)$; $\gamma \equiv 2\pi\Phi/\Phi_0$ with $\Phi \equiv Ha^2$; and $\{\Delta_i | i=1-8\}$ are the values of the superconducting pair-wave-function order parameter at the eight nodes of the cubic circuit. (Their precise definitions relative to the coordinate system are given in Fig. 1.) The gauge chosen is such that the vector potential \mathbf{A} has components $A_x = Hzn_y$, $A_y = H(xn_z - zn_x)$, and $A_z = 0$.

Setting the determinant of the above matrix equal to zero, we obtain a polynomial equation of fourth degree:

$$x^4 = a_3 x^3 + a_2 x^2 + a_1 x + a_0 = 0, \quad (2)$$

where $x \equiv \lambda^2$ and

$$a_3 = -12, \quad a_2 = 42 - 4[\cos(\gamma n_x) + \cos(\gamma n_y) + \cos(\gamma n_z)],$$

$$a_1 = 4\{\cos^2(\gamma n_x) + \cos^2(\gamma n_y) + \cos^2(\gamma n_z) - [\cos(\gamma n_x) + \cos(\gamma n_y) + \cos(\gamma n_z) - 2]^2 - 2 \cos(\gamma n_x) \cos(\gamma n_y) \cos(\gamma n_z) - 7\},$$

$$a_0 = [2 \cos(\gamma n_x) + 2 \cos(\gamma n_y) + 2 \cos(\gamma n_z) - 3]^2.$$

The four roots of this equation are obtained by solving the following two quadratic equations:

$$x^2 + [a_3/2 + (a_3^2/4 + u_1 - a_2)^{1/2}]x + u_1/2 + [(u_1/2)^2 - a_0]^{1/2} = 0, \quad (3a)$$

$$x^2 + [a_3/2 - (a_3^2/4 + u_1 - a_2)^{1/2}]x + u_1/2 - [(u_1/2)^2 - a_0]^{1/2} = 0, \quad (3b)$$

where

$$u_1 = \left[\frac{(c_0^2 + 4c_1^3/27)^{1/2} - c_0}{2} \right]^{1/3} + \left[\frac{-(c_0^2 + 4c_1^3/27)^{1/2} - c_0}{2} \right]^{1/3} - b_2/3,$$

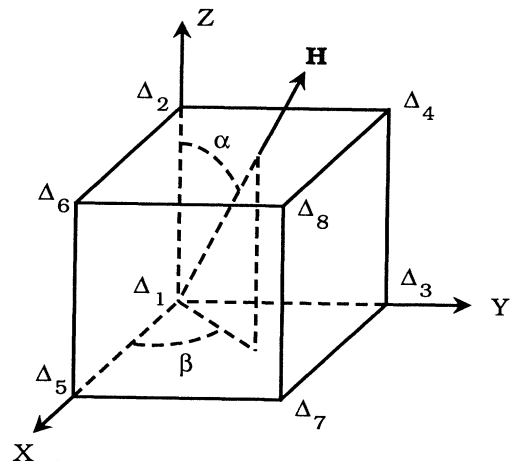


FIG. 1. The coordinate system used and the definition of $\{\Delta_i, i=1-8\}$ relative to the coordinate system.

with $c_1 = b_1 - b_2^3/3$, $c_0 = 2b_2^3/27 - b_1b_2/3 + b_0$, and $b_2 = -a_2$, $b_1 = a_1a_3 - 4a_0$, $b_0 = -(a_1^2 + a_0a_3^2 - 4a_0a_2)$. These four roots gives four positive values for $(a/\xi)^2$, the smallest one of which determines the phase boundary $T_c(\mathbf{H})$ of the circuit, where the dependence on the magnitude of \mathbf{H} enters through γ , and the dependence on the direction of \mathbf{H} enters through the directional cosines (n_x, n_y, n_z) . Since $\xi(T) = \xi(0)(1 - T/T_{c0})^{-1/2}$, the smallest a^2/ξ^2 obtained this way is directly proportional to the percent reduction of the transition temperature, $(1 - T_c/T_{c0})$.

The results are shown in the following 13 figures. In Figs. 2–6 the α dependence of $(a/\xi)^2$ is plotted for five values of β , viz., 0 , $\tan^{-1}(\frac{1}{6}) = 9.46^\circ$, $\tan^{-1}(\frac{1}{3}) = 18.44^\circ$, $\tan^{-1}(\frac{511}{800}) = 32.57^\circ$, and 45° , and each for five values of Φ/Φ_0 , viz., 0 , $\frac{1}{4}$, $\frac{1}{2}$, $\frac{3}{4}$, and 1 . Figures 7–11 are simply extensions of Figs. 2–6, respectively, to three larger values of Φ/Φ_0 , viz., 2 , 5 , and 10 . Note that the full range for α is 180° , but the curves have mirror symmetry about $\alpha = 90^\circ$, so only the range $\alpha = 0^\circ - 90^\circ$ needs to be presented. Also the full range for β is 360° , but the curves have 90° periodicity, and within each period, they have mirror symmetry about the midpoint, so only the range $\beta = 0^\circ - 45^\circ$ needs to be presented. These symmetries are, of course, those of a cube. (The same cubic symmetry also explains why there is a mirror symmetry in the curves in Figs. 2 and 7, which are both for $\beta = 0^\circ$, and that an asymmetry evolves in the two sequences of figures following these two figures which correspond to increas-

ing β toward 45° . Figure 1 ought to help the readers to see this point easily.) From these figures, it is seen that the dependence of the transition temperature on the two angles α and β becomes more sensitive and complex, as Φ/Φ_0 is increased to larger values beyond unity, so that even with five figures at five roughly equally spaced values of β , one must still struggle somewhat in order to visualize the continuous variation of the transition temperature with the angle β . On the other hand, for $\Phi/\Phi_0 < 1$, this dependence is much less complex, so one does not really need five figures to see this continuous variation. But five are given also in this case (in Figs. 2–6), so one can also see how the T_c -versus- α curve evolves as Φ/Φ_0 is increased, at several constant values of β , by combining Fig. 2 with Fig. 7, Fig. 3 with Fig. 8, etc.⁵ (For more on this Φ/Φ_0 dependence, see Figs. 12–14 below.)

In Figs. 12–14 we have plotted $(a/\xi)^2$ as a function of Φ/Φ_0 for three choices of the polar angles (α, β) . These three choices represent three distinct types of behavior of this dependence. The first choice (Fig. 12) is such that the directional cosines (n_x, n_y, n_z) are in the *rational* ratios 6:2:3. The curve is seen to be periodic with the period 7, which is nothing but the square root of $6^2 + 2^2 + 3^2$ —just what is needed to normalize (n_x, n_y, n_z) such that $n_x^2 + n_y^2 + n_z^2 = 1$. [This period, of course, does not have to be always an integer. For example, for $n_x:n_y:n_z = 1:2:3$, the period would be $(1^2 + 2^2 + 3^2)^{1/2} = \sqrt{14}$. We have chosen it to be an integer here, so it can

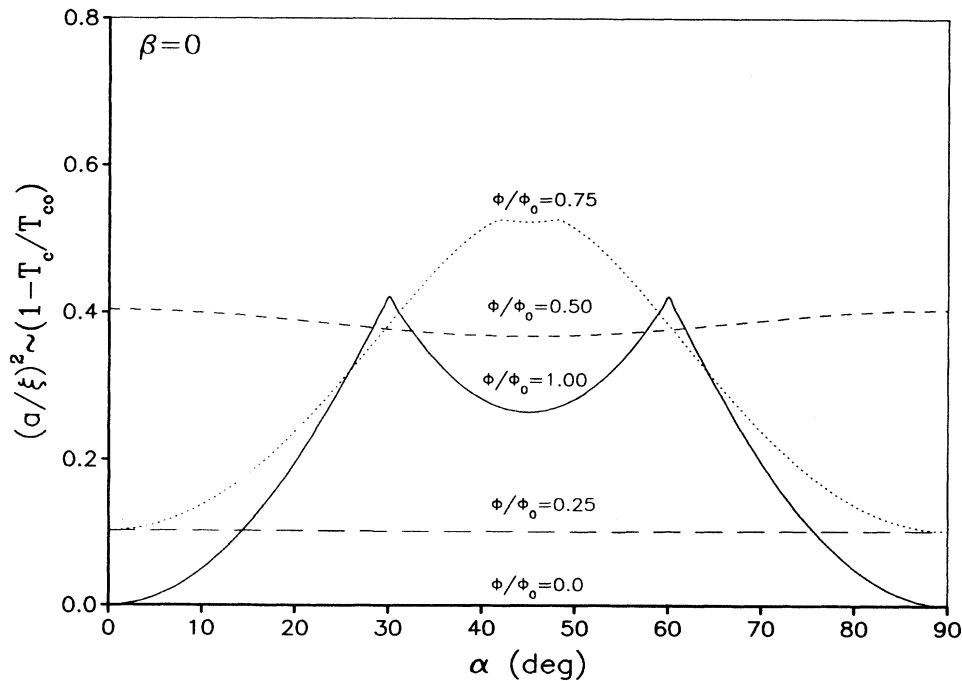


FIG. 2. Plot of $(a/\xi)^2 \sim (1 - T_c/T_{c0})$ as a function of α for $\beta=0$ and for five values of Φ/Φ_0 , viz., 0 , $\frac{1}{4}$, $\frac{1}{2}$, $\frac{3}{4}$, and 1 . The mirror symmetry about $\alpha=45^\circ$ in these curves simply reflects the mirror symmetry of the cube about the plane spanned by the two directions $(1,0,1)$ and $(0,1,0)$. This symmetry is gradually lost as β is increased from zero toward 45° , as is shown in the next four figures.

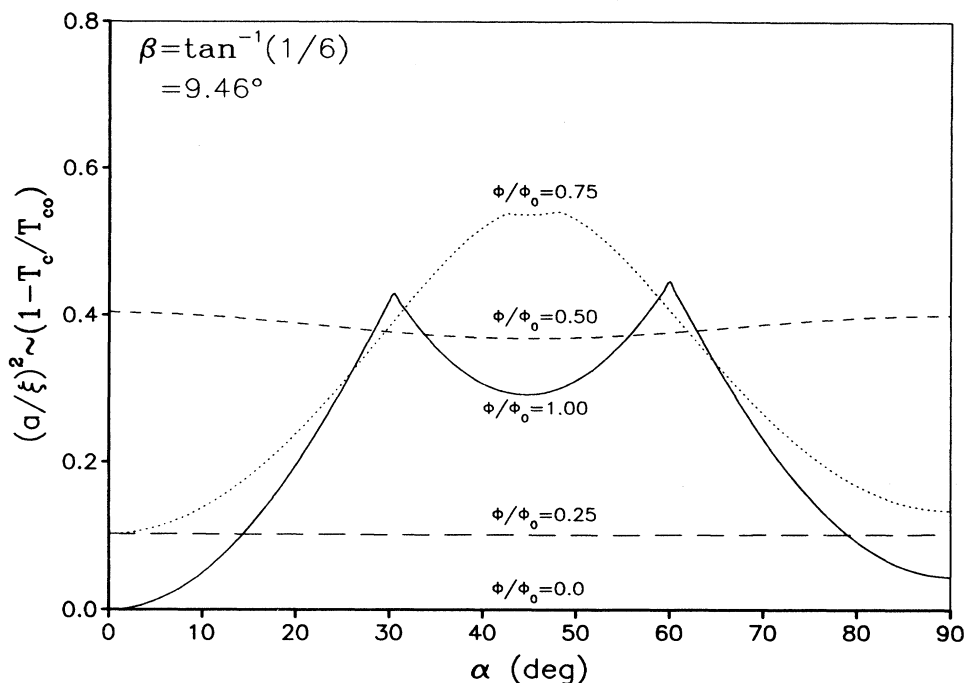


FIG. 3. Same as Fig. 2 except that $\beta = \tan^{-1}(1/6) = 9.46^\circ$.

be easily confirmed on the figure.] The second choice (Fig. 13) is such that (n_x, n_y, n_z) are in the partially rational ratios $2:1:\sqrt{3}$. The curve is then only quasiperiodic, and it also exhibits a beatlike phenomenon. This is because that the plotted quantity is a *nonlinear* combination of only *two* simple harmonic components of mutually in-

commensurate periods. Finally in Fig. 14 we have the third choice which is such that (n_x, n_y, n_z) are in the *totally irrational* ratios $\sqrt{5}:\sqrt{2}:\sqrt{3}$. In this case the curve is also only quasiperiodic, but it no longer exhibits any beatlike phenomenon, because it is now a nonlinear combination of *three* simple harmonic components of mutual-

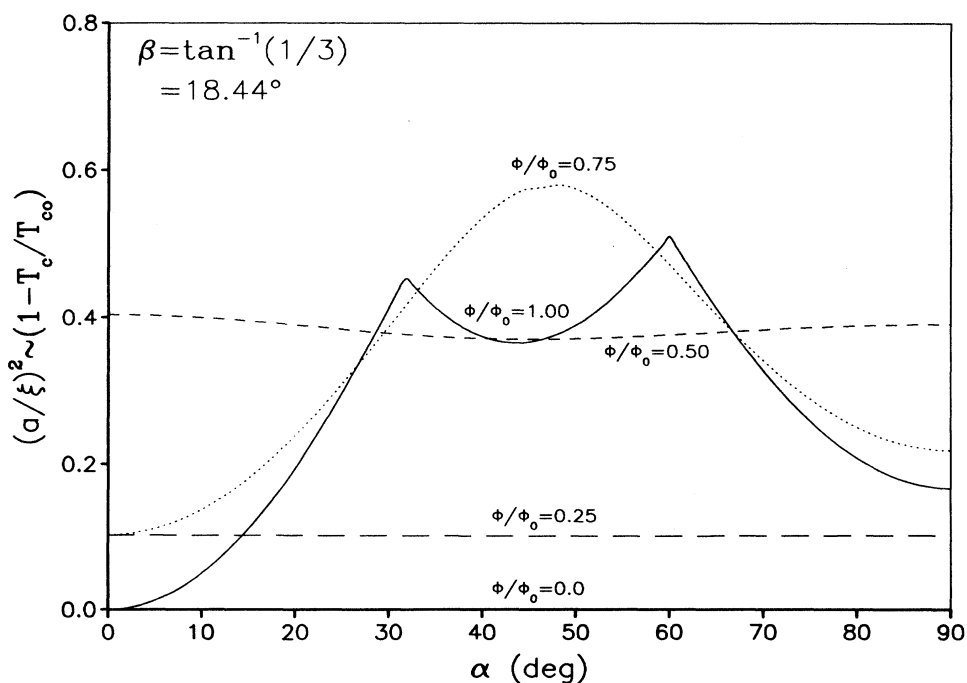


FIG. 4. Same as Fig. 2 except that $\beta = \tan^{-1}(1/3) = 18.44^\circ$.

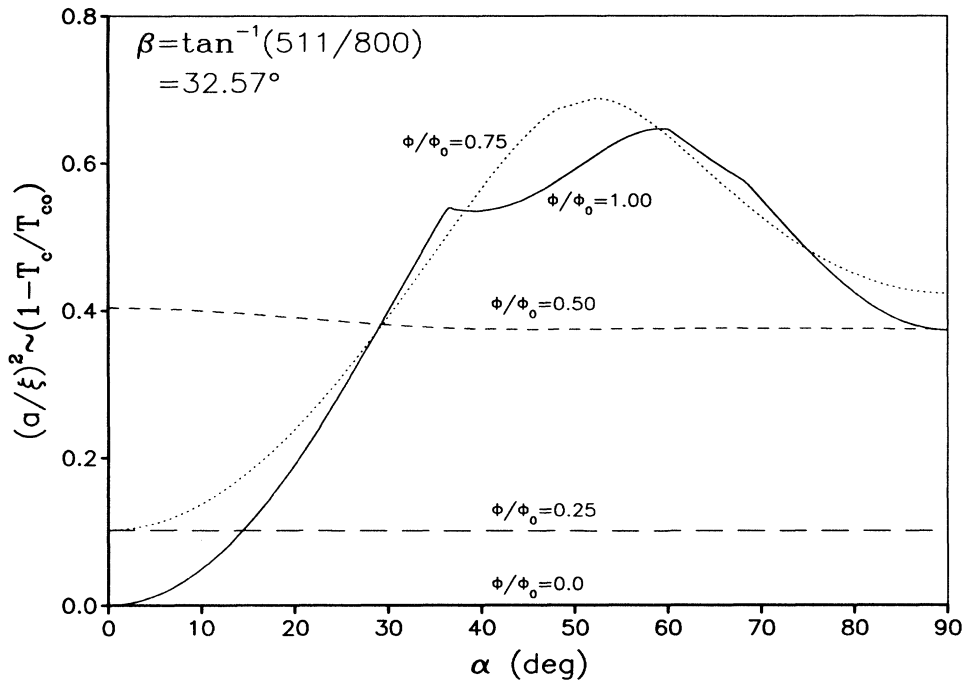


FIG. 5. Same as Fig. 2 except that $\beta = \tan^{-1}(\frac{511}{800}) = 32.57^\circ$.

ly incommensurate periods. [The periods are simply $1/n_x$, $1/n_y$, and $1/n_z$, so that the beat period in Fig. 13 is just $(n_x - n_z)^{-1} \approx 10.56$. See below for explanations.]

To digest the above results, it is important to realize first that even an *infinitesimal* change of the direction of

the applied magnetic field can switch the system among the three cases as represented in Figs. 12–14. (To see this, imagine an *infinite* cubic lattice of points. Then any direction which is pointing from a special lattice point designated as the origin toward any other lattice point is

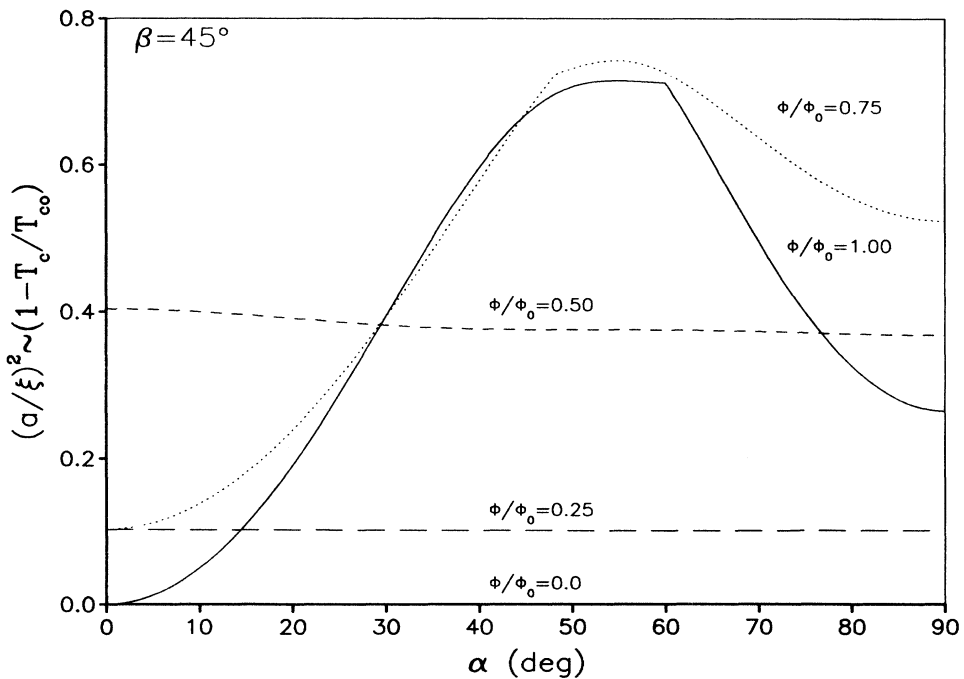


FIG. 6. Same as Fig. 2 except that $\beta = 45^\circ$. There is no need to go beyond 45° because of the fourfold symmetry of the cube, and the mirror symmetry of the cube about the plane of constant $\beta = 45^\circ$.

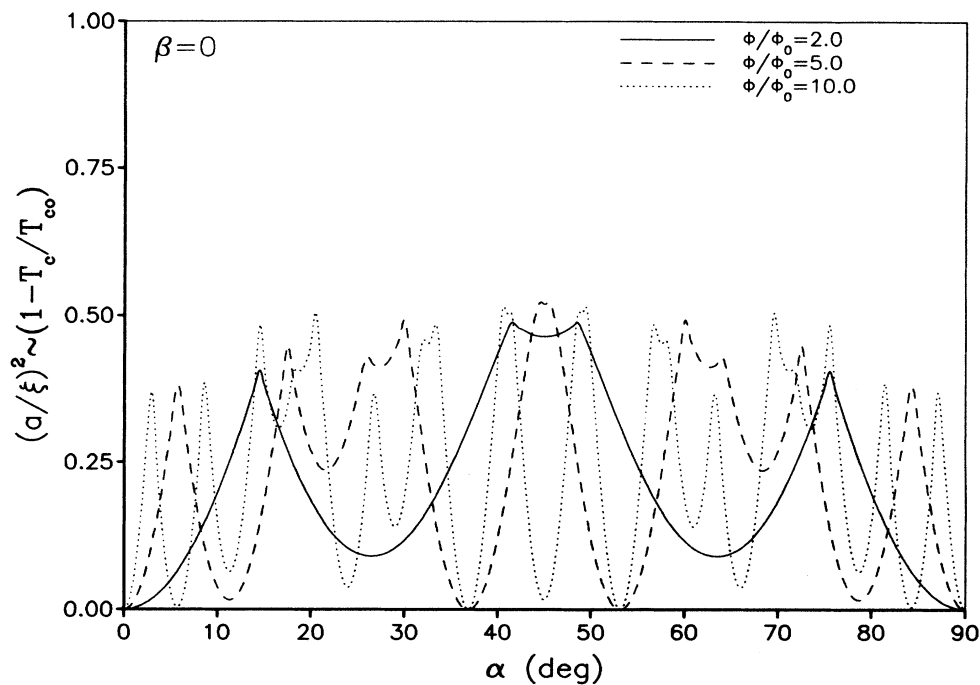


FIG. 7. Same as Fig. 2 except that it is now for three new values of Φ/Φ_0 , viz., 2, 5, and 10. One may combine this figure with Fig. 2 to visualize to some extent how the $(a/\xi)^2$ -vs- α curve changes (continuously) with Φ/Φ_0 at the given value of β .

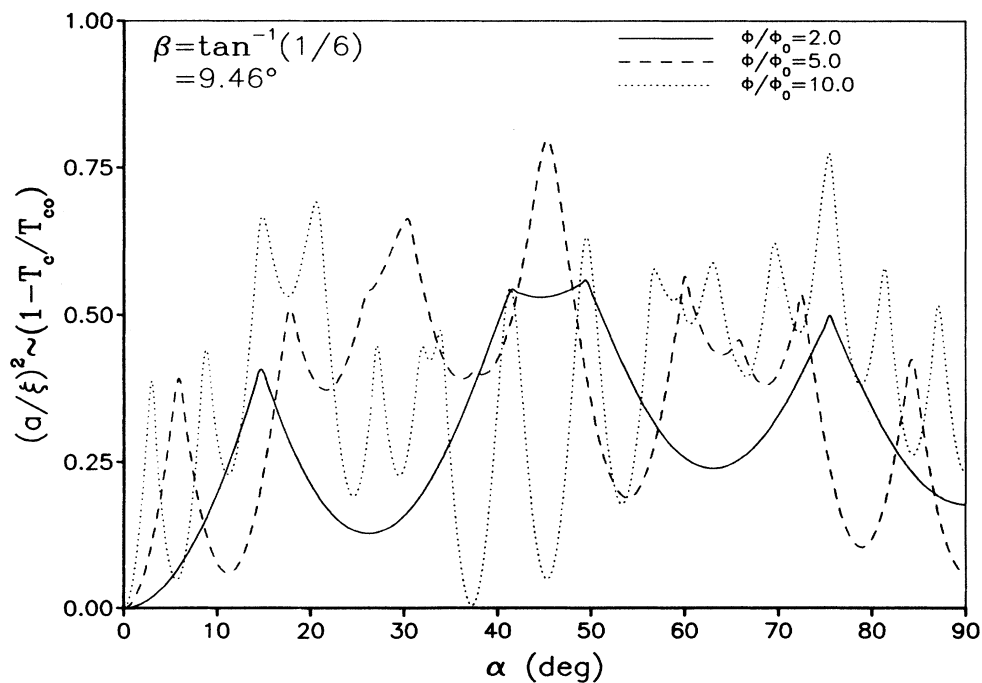


FIG. 8. Same as Fig. 7 except that $\beta = \tan^{-1}(1/6) = 9.46^\circ$ as in Fig. 3. One may combine this figure with Fig. 3 to visualize to some extent how the $(a/\xi)^2$ -vs- α curve changes (continuously) with Φ/Φ_0 at the given value of β .

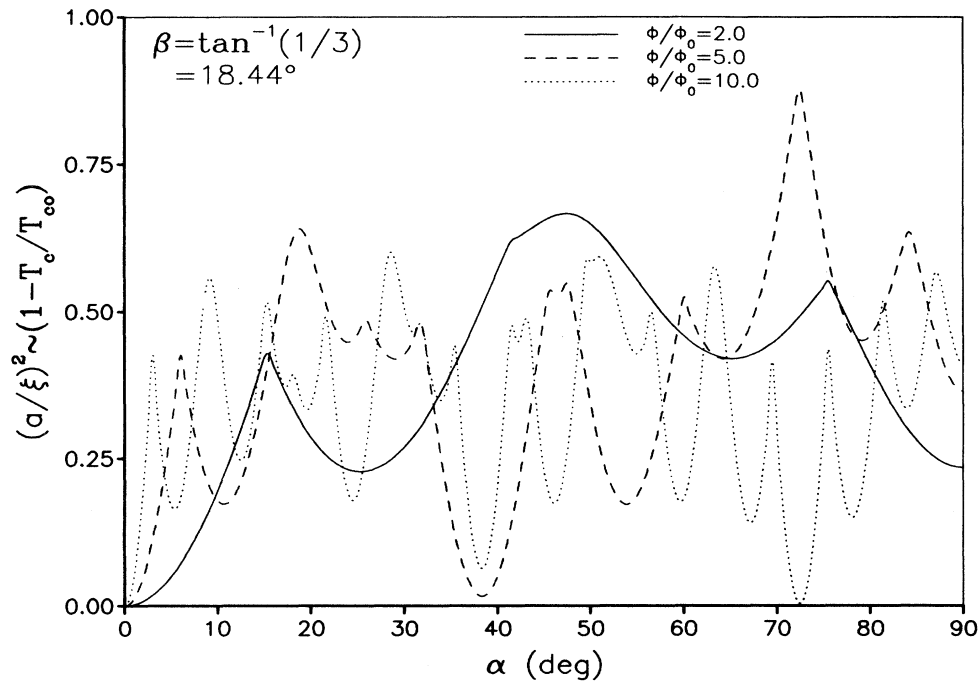


FIG. 9. Same as Fig. 7 except that $\beta = \tan^{-1}(1/3) = 18.44^\circ$ as in Fig. 4. One may combine this figure with Fig. 4 to visualize to some extent how the $(a/\xi)^2$ -vs- α curve changes (continuously) with Φ/Φ_0 at the given value of β .

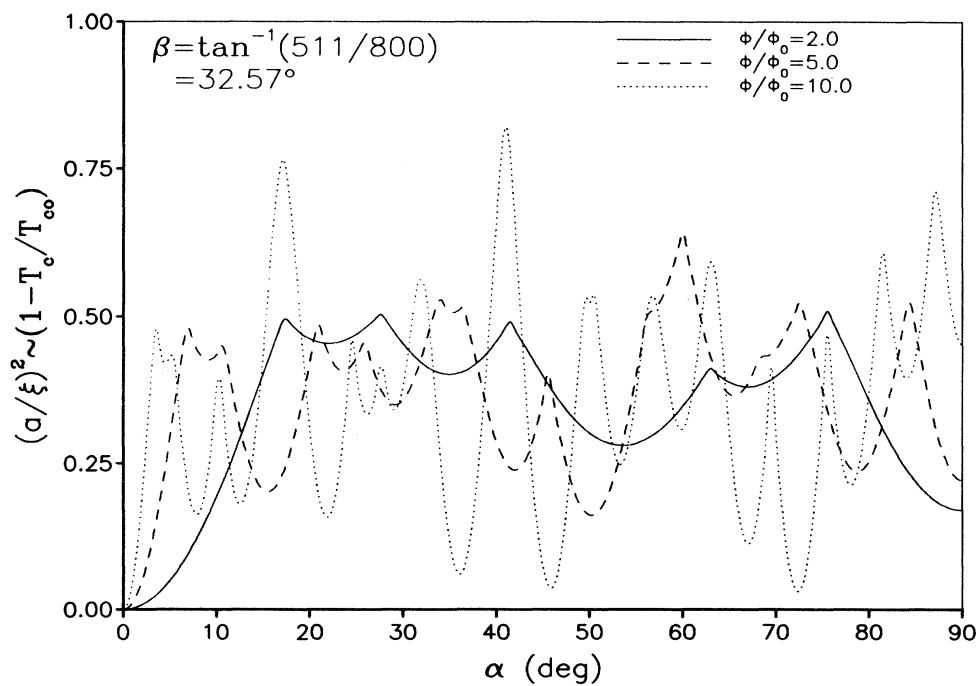


FIG. 10. Same as Fig. 7 except that $\beta = \tan^{-1}(511/800) = 32.57^\circ$ as in Fig. 5. One may combine this figure with Fig. 5 to visualize to some extent how the $(a/\xi)^2$ -vs- α curve changes (continuously) with Φ/Φ_0 at the given value of β .

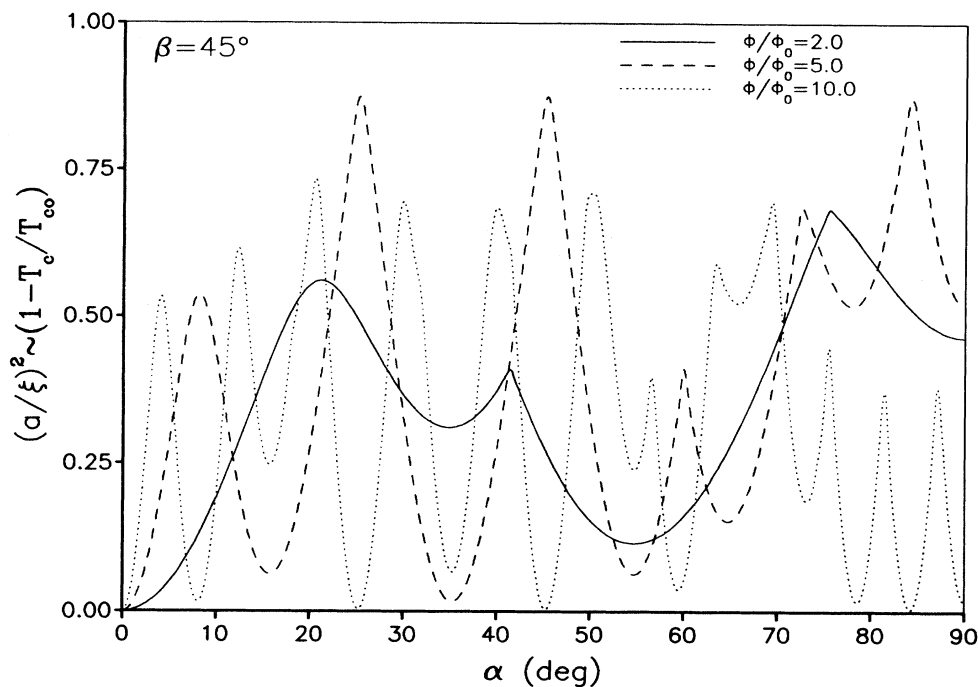


FIG. 11. Same as Fig. 7 except that $\beta=45^\circ$ as in Fig. 6. One may combine this figure with Fig. 6 to visualize to some extent how the $(a/\xi)^2$ -vs- α curve changes (continuously) with Φ/Φ_0 at the given value of β .

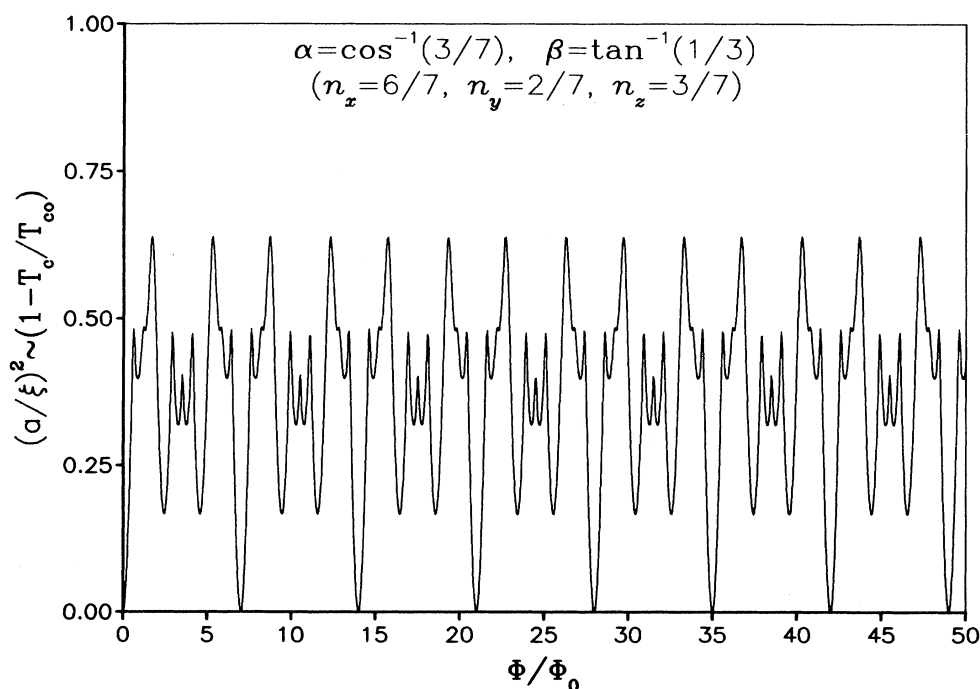


FIG. 12. Plot of $(a/\xi)^2 \propto (1 - T_c/T_{c0})$ as a function of Φ/Φ_0 for the special choice of the polar angles α and β as given, which is such that the directional cosines of the applied magnetic field are in the rational ratios 6:2:3. The curve is seen to be periodic with the period 7, which is the normalizing denominator of the directional cosines. This is because the three frustration parameters $n_x\Phi/\Phi_0$, $n_y\Phi/\Phi_0$, and $n_z\Phi/\Phi_0$ are all defined modulo unity, which means that whenever the external magnetic field vector is such that the fluxes through the six faces of the cube are all equal to integer multiples of the flux quantum, the transition temperature of the circuit should become unaffected by the presence of the external magnetic field, due to the absence of frustration in any closed path in the circuit.

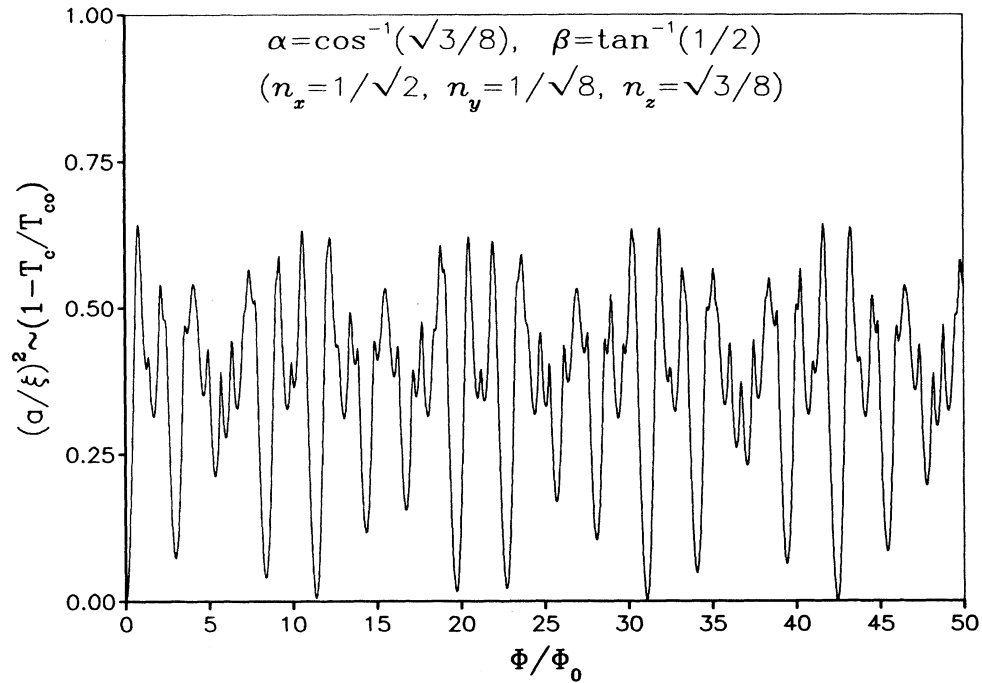


FIG. 13. Same as Fig. 12 except that the directional cosines are now in the partially rational ratios $2:1:\sqrt{3}$. In this case $(1 - T_c/T_{c0})$ can no longer drop to exactly zero at any finite field value, due to the impossibility of satisfying the zero-frustration condition at any finite field, although it can still sometimes come quite close to it. See the text for the explanation of the beatlike structure which is clearly visible in this figure.

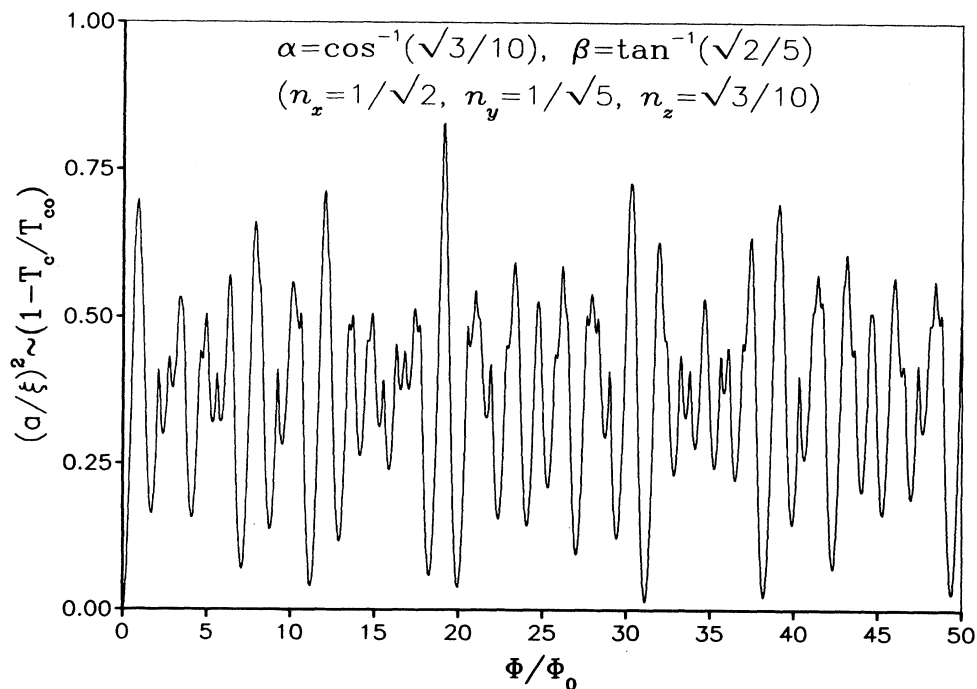


FIG. 14. Same as Fig. 12 except that the directional cosines are now in the totally irrational ratios $\sqrt{5}:\sqrt{2}:\sqrt{3}$. Here again $(1 - T_c/T_{c0})$ cannot drop to exactly zero at any finite field value, but furthermore even the beatlike structure of the previous case is no longer present. See the text for explanation.

characterized by directional cosines that are in rational ratios. Clearly, between any two such directions there is at least another such direction, so there must exist a countable infinity of such *rational* directions within any angular neighborhood, however small, of any given direction, interspersed within an uncountable infinity of partially rational or totally irrational directions.) Thus we see that the transition temperature of a cubic superconducting circuit is a very sensitive function of both the magnitude and the direction of the applied magnetic field, especially at large Φ/Φ_0 .

The rich structure in the phase boundary of *any* superconducting network is due to the frustration effect,⁶ which can suppress the superconducting transition temperature. The amount of frustration imposed on a single closed superconducting loop is measured by the deviation from any integer value of the magnetic flux through the loop in units of the flux quantum, due to the Aharonov-Bohm effect.⁷ For example, the phase boundary of a two-dimensional infinite square superconducting network in a perpendicular magnetic field H is periodic in Φ/Φ_0 with the period unity, where Φ is the flux through each square unit cell, and within each period the phase boundary has cusps of various sizes at all rational values of Φ/Φ_0 ,⁸ precisely because at any integer values of Φ/Φ_0 no closed loops in the network are frustrated, whereas at any rational values of Φ/Φ_0 , only some closed loops of the networks are not frustrated. Now a cubic superconducting circuit has square loops of area a^2 facing each of the three axes x , y , and z . Thus the relevant frustration parameters are $n_x\Phi/\Phi_0$, $n_y\Phi/\Phi_0$, and $n_z\Phi/\Phi_0$, which correspond to the amounts of flux passing through the three types of square loops measured in units of the flux quantum, respectively, when the direction of the magnetic field is such that its directional cosines are given by (n_x, n_y, n_z) . Thus all of these three frustration parameters prefer to have integer values. When they all do have integer values, no frustration would be present in the circuit at all. Then $T_c(\mathbf{H})$ must become equal to T_{c0} , and the $(a/\xi)^2$ curve must drop to zero, as is exemplified by all the biggest dips in Fig. 12. This situation also occurs in several places in Figs. 2–11. For example, in Fig. 7, the dashed and dotted curves both dip to zero at $\alpha = \cos^{-1}(\frac{4}{5}) = 36.87^\circ$ and $\cos^{-1}(\frac{3}{5}) = 53.13^\circ$, corresponding to (n_x, n_y, n_z) equal to $(\frac{4}{5}, 0, \frac{3}{5})$ and $(\frac{3}{5}, 0, \frac{4}{5})$, respectively. Note that for these two curves, Φ/Φ_0 are multiples of 5, but not the third curve (i.e., the solid curve) in the same figure which also does not drop to zero at these values of α , as expected. In all of the plotted curves, all major dips which do not quite touch the horizontal axis can also be understood as (n_x, n_y, n_z) all reaching *almost* integer values. For example, in Fig. 9, the dotted curve almost touched the horizontal axis at $\alpha \approx 72.4^\circ$, where $(n_x, n_y, n_z) \approx (0.904, 0.301, 0.302)$, which, when multiplied by $\Phi/\Phi_0 = 10$, becomes all very near integer values. In the same figure, the dashed curve reaches a major *maximum* at the same value of α [corresponding to a major local *minimum* in $T_c(\mathbf{H})$] because for $\Phi/\Phi_0 = 5$, all three frustration parameters become very near *half-integer* values, corresponding to *maximum frustration*. Many

major minima and maxima in the plotted curves can be understood in this way, but we shall not go through all of them here. The minor minima and maxima in these curves are harder to understand in detail. Some of them may be caused by minimum or maximum frustration in a larger loop which encompasses two or three faces of the cube. Figures 2–14 all reveal that all minima of all curves are quadratic, whereas some maxima of some curves are cusplike. Such features are typical of circuits containing only a finite number of links, as is already shown to be the case in two-dimensional networks. (See, in particular, the work of Rammal *et al.* in Ref. 2)

Extensions of this study to some multicube circuits and even to an infinite cubic network in three dimensions should be interesting, and are presently under consideration. The solutions to these extensions, however, must resort to much more numerical work, and probably cannot be as accurate or complete as the present study of a single-cube circuit. However, from our general understanding of infinite, *two-dimensional*, periodic networks, we expect that, if the single-cube circuit considered here is extended to a three-dimensional *infinite* cubic network, all minima of a^2/ξ^2 (corresponding to maxima of T_c) as a function of α , β , or Φ/Φ_0 , will become cusp shaped, and that new smaller cusps (or slope discontinuities) will show

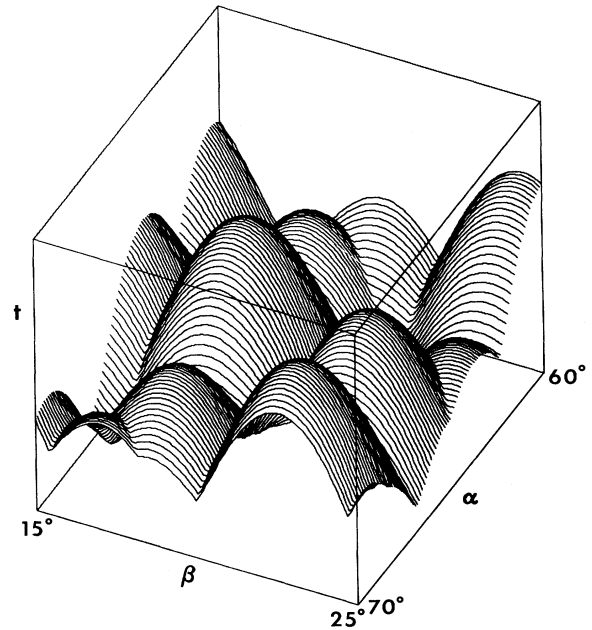


FIG. 15. Three-dimensional plot of $t \equiv T_c(\mathbf{H})/T_{c0}$ as a function of α and β (the polar angles of \mathbf{H}), for the range $60^\circ < \alpha < 70^\circ$ and $15^\circ < \beta < 25^\circ$, at $\Phi/\Phi_0 = 14$. The cubic circuit is assumed to be made of a type of aluminum film with $\xi_0 = 0.3 \mu\text{m}$ and $a = 3 \mu\text{m}$. The upward axis is t at an arbitrary scale. The axis pointing toward the lower left is α for the range given, and the axis pointing toward the lower right is β for the range given. The rectangular frame is drawn to show the viewing direction. The major-peak value of t at $\alpha = 64.62^\circ$ and $\beta = 18.43^\circ$ is unity, and the lowest value of t within this range is 0.991 534 . . .

up at values of α , β , and Φ/Φ_0 where all three frustration parameters are equal to rational fractions. (For fields along the principal directions of the cube, this can already be demonstrated in a way much similar to the corresponding solution of a infinite, two-dimensional, square network.)

In summary, we have presented an exact analytic calculation of the phase boundary of a cubic superconducting circuit made of 12 identical thin superconducting straight line segments, in an external magnetic field of arbitrary magnitude and direction. This is probably the first and also one of the simplest calculation of its kind which demonstrates the sensitive and complex dependence of the phase boundary of a *three-dimensional* superconducting network on both the magnitude *and the direction* of an external magnetic field. The sensitive directional dependence is particularly interesting and should have some applicational value. For example, if the magnitude and the directional cosines of an applied magnetic field are all preset at such values as to hold the T_c of a cubic superconducting circuit at one of its major maxima, and the temperature T is kept constant at a value just below this $T_c(\mathbf{H})$, then *any* slight change of the relative orientation between the magnetic field and the cubic circuit should lead to a large increase in the resistance of the circuit which clearly can be used in a feedback circuit to control the orientation of a device or instrument. To help the reader visualize this point, we have given in Fig. 15 a three-dimensional plot of $T_c(\mathbf{H})/T_{c0}$ as a function of both α and β in the *small* range $60^\circ < \alpha < 70^\circ$ and $15^\circ < \beta < 25^\circ$, assuming that $\Phi/\Phi_0 = 14$, and that the circuit is made of some type of aluminum film with $\xi_0 = 0.3 \mu\text{m}$ and $a = 3 \mu\text{m}$. We

choose this region to plot $T_c(\mathbf{H})/T_{c0}$ because we know from Fig. 12 that it has a major peak of value unity at $\alpha = \cos^{-1}(\frac{3}{7}) \approx 64.62^\circ$ and $\beta = \tan^{-1}(\frac{1}{3}) \approx 18.43^\circ$, which correspond to a point in the chosen range, for any Φ/Φ_0 which is an integer multiple of 7, such as 14. The peak will actually be narrower for higher multiples of 7 for Φ/Φ_0 , but more peaks will then show up in this narrow range of α and β , so that one would have to plot an even smaller range of these angles in order to show clearly the vicinity of one major peak. One can therefore understand why we do not attempt to present a three-dimensional plot of $T_c(\mathbf{H})/T_{c0}$ for the *entire* range of the two angles.

Other applications of this cubic superconducting circuit might include the accurate determination of the magnitude *and direction* of an unknown feeble external magnetic field. For any of such applications a network containing a large number of cubes can definitely offer more sensitivity than a single-cube circuit, much like the improvement from a double-slit interferometer to a grating. But the fabrication of any such three-dimensional circuits or networks is probably still a serious challenge to the present-day technology, so one probably should start by trying to make the simplest configuration first, viz., a single-cube circuit, and perhaps test its characteristics by comparing it with the present calculation (probably also with much difficulty due to very small signal associated with a small circuit).

One of us (C.R.H.) would like to acknowledge some support from the Texas Center for Superconductivity at the University of Houston, and National Tsing-Hua University of Taiwan, Republic of China.

¹See, for example, B. Pannetier, J. Chaussy, R. Rammal, and J. C. Villegier, Phys. Rev. Lett. **53**, 1845 (1984); J. M. Gordon, A. M. Goldman, J. Maps, D. Costello, R. Tiberio, and B. Whitehead, *ibid.* **56**, 2280 (1986); A. Behrooz, M. J. Burns, H. Deckman, D. Levine, B. Whitehead, and P. M. Chaikin, *ibid.* **57**, 368 (1986); A. Behrooz, M. J. Burns, D. Levine, B. Whitehead, and P. M. Chaikin, Phys. Rev. B **35**, 8396 (1987); P. Santhanam, C. C. Chi, and W. W. Molzen, *ibid.* **37**, 2360 (1988); P. Santhanam and C. C. Chi, Physica B **152**, 129 (1988).

²See, for example, P. G. de Gennes, C. R. Acad. Sci. Series II **292**, 9 (1981); **292**, 279 (1981); J. Simonin, D. Rodrigues, and A. López, Phys. Rev. Lett. **49**, 944 (1982); J. Simonin, C. Wiecko, and A. López, Phys. Rev. Lett. B **28**, 2497 (1983); J. Simonin and A. López, Phys. Rev. Lett. **56**, 2649 (1986); H. J. Fink, A. López, and R. Maynard, Phys. Rev. B **26**, 5237 (1982); S. Alexander, *ibid.* **27**, 1541 (1983); S. Alexander and E. Halevi, J. Phys. (Paris) **44**, 805 (1983); R. Rammal, T. C. Lubensky, and G. Toulouse, Phys. Rev. B **27**, 2820 (1983); S. Teitel and C. Jayaprakash, J. Phys. Lett. **46**, L33 (1985); F. Nori, Q. Niu, E. Franklin, and S.-J. Chang, Phys. Rev. B **36**, 8338 (1987); F. Nori and Q. Niu, *ibid.* **37**, 2364 (1988); C.-R. Hu, *ibid.* **35**, 5294 (1987); C.-R. Hu and R. L. Chen, *ibid.* **37**, 7907 (1988); P. Santhanam and C. C. Chi, *ibid.* **38**, 11 843

(1988); C. C. Chi, P. Santhanam, and P. E. Blöchl, *ibid.* **42**, 76 (1990); C. M. Soukoulis, G. S. Grest, and Q. Li, *ibid.* **38**, 12 000 (1988).

³R. Rammal, T. C. Lubensky, and G. Toulouse, previous reference; C.-R. Hu, previous reference.

⁴M. Jeffery, C. Green, S. Tyagi, and G. Gilmore, Int. J. Mod. Phys. B **2**, 1399 (1988); Phys. Rev. B **39**, 9054 (1989).

⁵One might think that three-dimensional plots of $T_c(\alpha, \beta)$ at a sequence of values for Φ/Φ_0 will do a better job in revealing these continuous dependences, but we find that such plots cannot be made sufficiently quantitative to support our discussions about the positions of the maxima and minima in these curves, and many features will even be hidden behind other features and not be revealed. Also, we think that treating α and β as Cartesian coordinates in a three-dimensional plot is very misleading, since they are actually defined on a unit sphere. Three-dimensional plots on the surface of a sphere is of course theoretically possible, but we have not figured out a good way to do it so that all the important features of the curves can be revealed.

⁶G. Toulouse, Commun. Phys. **2**, 115 (1977); see also, Pannetier *et al.* (Ref. 1); Hu and Chen (Ref. 2).

⁷Y. Aharonov and D. Bohm, Phys. Rev. **115**, 485 (1959).

⁸See Pannetier *et al.* (Ref. 1) Rammal *et al.* (Ref. 2).